Applied Surface Science 257 (2011) 6314–6319

Contents lists available at ScienceDirect

Applied Surface Science

journal homepage: www.elsevier.com/locate/apsusc

Laser energy density, structure and properties of pulsed-laser deposited zinc oxide films

M.G. Tsoutsouva[b], C.N. Panagopoulos[b], M. Kompitsas[a,*]

[a] National Hellenic Research Foundation, Theoretical and Physical Chemistry Institute, Vasileos Konstantinou Ave. 48, Athens 11635, Greece
[b] Laboratory of Physical Metallurgy, National Technical University of Athens, Zografos, Athens 15780, Greece

ARTICLE INFO

Article history:
Received 8 November 2010
Received in revised form 15 February 2011
Accepted 15 February 2011
Available online 22 February 2011

Keywords:
ZnO films
Nanosecond pulsed laser deposition
Structural
Optical and electrical properties
Laser energy density dependence

ABSTRACT

Zinc oxide thin films were deposited on soda lime glass substrates by pulsed laser deposition in an oxygen-reactive atmosphere at 20 Pa and a constant substrate temperature at 300 °C. A pulsed KrF excimer laser, operated at 248 nm with pulse duration 10 ns, was used to ablate the ceramic zinc oxide target. The structure, the optical and electrical properties of the as-deposited films were studied in dependence of the laser energy density in the 1.2–2.8 J/cm^2 range, with the aid of X-ray Diffraction, Atomic Force Microscope, Transmission Spectroscopy techniques, and the Van der Pauw method, respectively. The results indicated that the structural and optical properties of the zinc oxide films were improved by increasing the laser energy density of the ablating laser. The surface roughness of the zinc oxide film increased with the decrease of laser energy density and both the optical bang gap and the electrical resistivity of the film were significantly affected by the laser energy density.

1. Introduction

Zinc oxide (ZnO) is a transparent wide band gap semiconducting material having a variety of interesting applications, such as for gas sensors, piezoelectric devices, surface acoustic wave devices, field effect transistors, solar cells, catalysts, and others [1–3].

Many techniques are applied for the growth of ZnO films, including sputtering, thermal evaporation, chemical vapor deposition (CVD), sol–gel, molecular beam epitaxy (MBE) and electrodeposition. Besides the above listed techniques, pulsed laser deposition (PLD) has emerged as an efficient technique for growing ZnO films, as it provides several advantages compared to others. The composition of the films grown by PLD is quite close to that of the target material, even for a multicomponent target. Pulsed laser deposited films crystallize at lower substrate temperatures relative to other physical vapor deposition (PVD) techniques; this is due to the high kinetic energies (>1 eV) of the ejected atoms and ionized species in the laser-produced plasma [4]. Due to the low crystallization temperature, PLD is also used for the growth of films even on organic substrates [5], a fact that is essential for fabrication of flexible flat-panel displays.

Most of the works that deal with pulsed laser deposited ZnO films focus on the influence that the deposition parameters, such as the reactive gas pressure and substrate temperature [6] have on the film properties. In the present investigation, ZnO films were grown using the PLD technique and the influence of the ablating laser energy density (in J/cm^2) on the crystalline structure, the surface morphology, optical transmission and electrical resistivity of the films was investigated. In particular, the laser pulse energy was constant at 65 mJ/p (maximum pulse energy available) and the distance of the focusing lens from the target was changed. To the best of our knowledge, only very few investigations in the past have focused on this aspect during film growth [7–10]. However, their experimental conditions were very different from ours.

2. Experimental

ZnO thin films were deposited in a high vacuum chamber that was initially evacuated to a base pressure at 10^{-4} Pa. A UV pulsed KrF excimer laser, operated at 248 nm with a repetition rate of 10 Hz and pulse duration 10 ns, was used to ablate the target, a ceramic ZnO disc (99.9% of purity) with 1.2 cm in diameter and 0.5 cm thickness. To avoid fast drilling, the target was mounted on a vacuum compatible, computer-controlled XY-stage and performed a meander-like movement. The laser beam was focused through a 70 cm focal lens onto the target at a 45° angle of incidence. The substrates were microscope soda lime glass slides; they were cleaned for 10 min in an ultrasonic bath with acetone before being loaded into the chamber and placed parallel to the target surface at a distance of 5 cm. For all depositions, the oxygen pressure and the deposition time were constant at 20 Pa in dynamic flow and

* Corresponding author. Tel.: +30 2107273 834; fax: +30 2107273 794.
E-mail address: mcomp@eie.gr (M. Kompitsas).
URL: http://www.laser-applications.eu (M. Kompitsas).

0169-4332/$ – see front matter © 2011 Elsevier B.V. All rights reserved.
doi:10.1016/j.apsusc.2011.02.073

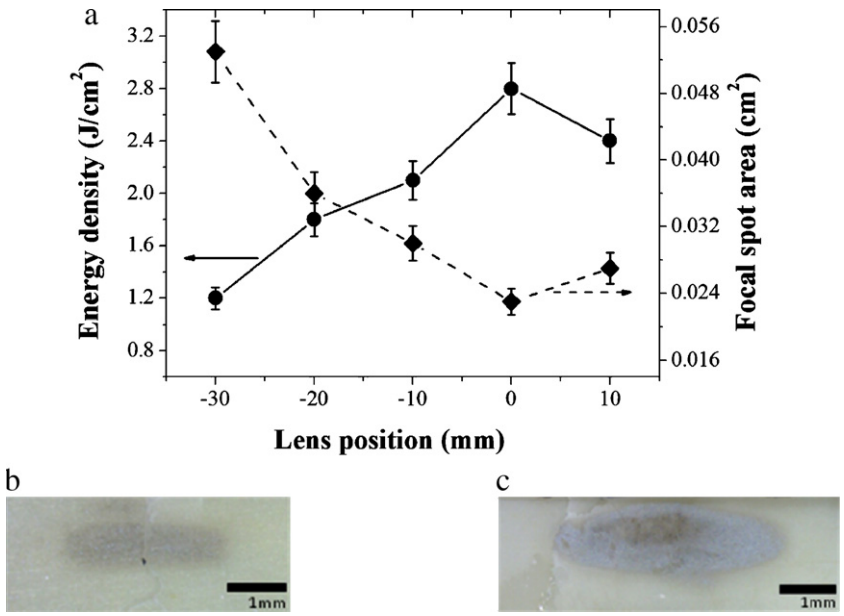

Fig. 1. (a) The calculated laser energy density as a function of the relative lens position. The position 0 corresponds to the lens focal distance. The measured laser spot area (single shot) is shown for (b) the highest and (c) the lowest energy density.

90 min, respectively. At a constant substrate temperature of 300 °C, five ZnO films were prepared with of 1.2, 1.8, 2.1, 2.4, and 2.8 J/cm^2 laser energy density.

The structure of the deposited ZnO films were investigated with X-ray Diffraction (XRD, Bruker D8 Focus) technique in Bragg–Brentano geometry, using the Cu-Kα_1 line (λ = 1.5406 Å). The root mean square (RMS) roughness of the films was measured with the aid of an Atomic Force Microscope (AFM, DME Dualscope DS95) and the optical transmittance, by Spectrophotometry (Perkin Elmer Lambda 19) in the 300–800 nm wavelength range. The electrical resistivity of the films was measured with the 4-point Van der Pauw method. All measurements were performed at room temperature. The given values of various parameters are the average values of four independent experiments.

3. Results and discussion

In previous investigations [8–10], the laser energy density varied by changing the laser pulse energy while keeping constant the distance of the focusing lens from the target. In the present work, the pulse energy was maintained constant at 65 mJ/p measured before the target inside the chamber and the irradiated area was varied by changing the lens distance from the ZnO target. In Ref. [7] the focusing lens distance was also changed, however, no optical and electrical results were reported; furthermore, their laser properties as well as the deposition parameters were very different from ours. In particular, no energy density values were given in Ref. [7].

The measurements of the (single pulse) laser spots were performed on a clear surface of the ceramic target and observed with an optical microscope. Fig. 1 presents the measured spot area for the highest and lowest energy density as well as the calculated energy density as a function of the lens position, relative to the position of the minimal spot area. As expected, the spot area is minimal in the focus position and increases when moving away from it.

3.1. Structure

Fig. 2 shows the X-ray diffraction pattern of the ZnO thin films deposited on glass substrates, for five different energy density values (1.2, 1.8, 2.1, 2.4 and 2.8 J/cm^2) and at constant substrate temperature (300 °C) and oxygen pressure (20 Pa). From this figure, it is evident that for all the applied laser energy densities the ZnO samples were crystalline and *c*-axis (0 0 2) oriented.

In Fig. 3 the Bragg angle of ZnO (0 0 2) diffraction peak (*a*), the full width at half maximum (FWHM) (*b*) and the peak intensity (*c*) are plotted as a function of the energy density. From this figure, it

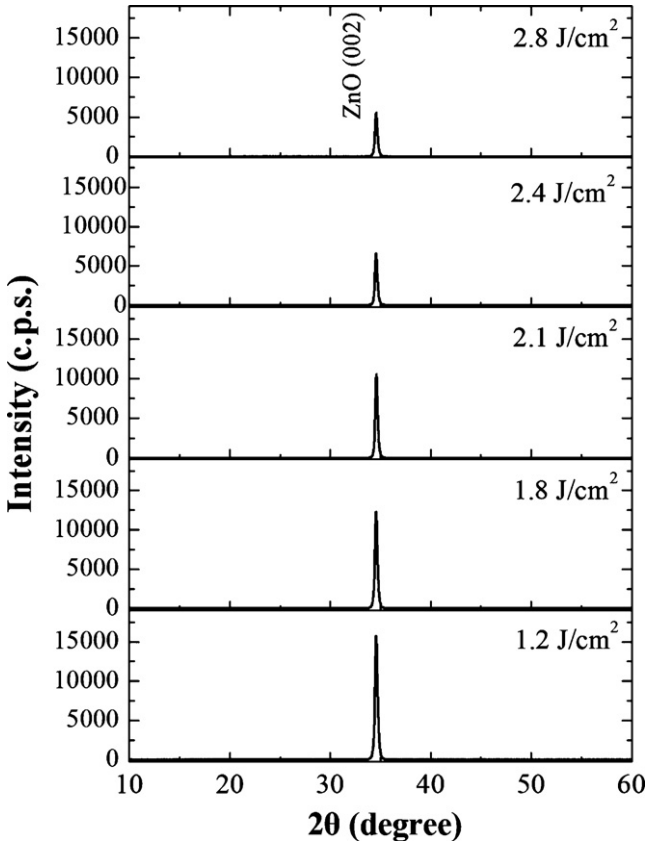

Fig. 2. X-ray diffraction pattern of ZnO thin films deposited at various laser energy densities.

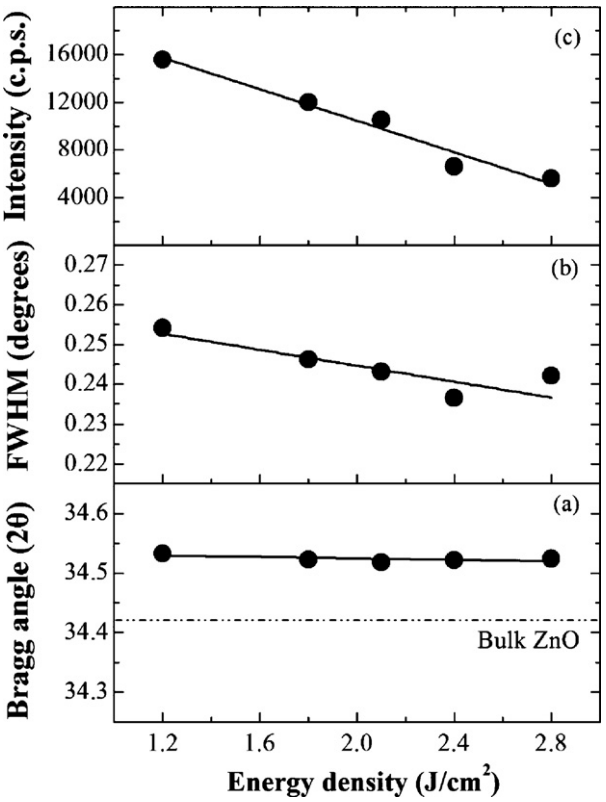

Fig. 3. (a) Bragg angle of the (0 0 2) diffraction peak, (b) FWHM and (c) intensity as a function of laser energy density.

results that the Bragg angle is not depending on the energy density values of this experiment and that is systematically larger than the angle of the ZnO bulk. This is an indication of tensile stresses inside the film. Such stresses correlate with the PLD technique applied here as they were also observed previously [8]. The FWHM decreases slightly with increasing energy density, resulting to a small increase of crystallite size of ZnO films. Similar observations were made [8,9] when the pulse energy was changed instead of the focal lens position. Furthermore, the peak intensity is decreasing with the laser energy density. This correlates with the decrease of the film thickness [8,9], see Fig. 7b.

The average grain size (Fig. 4) of the ZnO films grown with different laser energy density is calculated according to the following

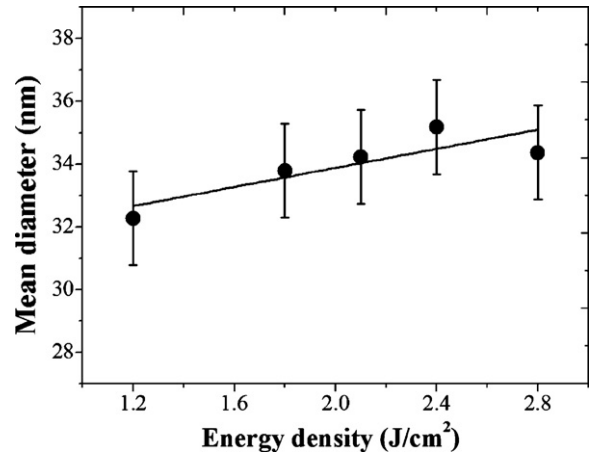

Fig. 4. The mean grain diameter of the ZnO films grown at different laser energy densities.

Debye–Scherrer equation:

$$D = \frac{0.94\lambda}{B\cos\theta} \quad (1)$$

where λ, θ and B are the X-ray wavelength (0.15405 nm), the Bragg diffraction angle and the peak width, respectively.

From this figure, it follows that the increase of energy density from 1.2 to 2.8 J/cm^2 increases the mean grain size of crystalline ZnO. An explanation of this phenomenon could be that by increasing the energy density, both the plasma density and the plasma kinetic energy increase. When the species (ions, neutrals and clusters) of the plasma arrive at the surface of the substrate, the kinetic energy of the deposited adatoms acquire higher diffusion, which results to the coalescence of grains and particles. Fig. 5(a–e) shows the AFM images (10 μm × 10 μm scanning range) of the ZnO films deposited with different energy density. The structures size that appears apparently larger than that of the XRD results may be due to the finite size of the AFM tip as well as to clusters formed on the film surface. Fig. 6 shows the variation of the root-mean-square (RMS) surface roughness as a function of the laser energy density for the ZnO films as it results from the AFM images and indicates a smoother surface.

From Figs. 5 and 6, it is obvious that the RMS surface roughness decreases with increasing incident laser energy density. This observation may be explained by the assumption that the increase of laser density leads to the better organization of the deposited adatoms on the various layers of the grown oxide.

3.2. Optical properties

Fig. 7(a and b) shows the optical transmittance spectra and the thickness of the ZnO films deposited with different laser energy density, respectively.

The thickness d of the ZnO films was estimated from two successive maxima or minima in the transmittance spectrum, according to the following equation [11]:

$$d = \frac{M \times \lambda_1 \times \lambda_2}{2(n(\lambda_1) \times \lambda_2 - n(\lambda_2)) \times \lambda_1} \quad (2)$$

where M is the number of oscillations between the two extremes (M = 1 between two consecutive maxima or minima), $n(\lambda_1)$, $n(\lambda_2)$ are the indices of refraction and λ_1, λ_2 are the corresponding wavelengths.

The indices of refraction, $n(\lambda_1)$ and $n(\lambda_2)$, were determined according to the following equation taken from Ref. [12]:

$$n(\lambda) = \sqrt{1 + \frac{A\lambda^2}{\lambda^2 - B^2}} \quad (3)$$

where for ZnO: A = 2.51 and B = 0.205 μm.

All deposited films in this work show a high average transmission up to 95% that depends slightly on the laser energy density. A slight decrease of the optical transmittance for lower laser energy density could be attributed to the increase of film thickness (Fig. 7b) [13,14], the decrease of grain size and the increase of the RMS roughness of the ZnO films (Fig. 6) as a result to multiple reflections on the film surface.

The film thickness on the laser energy density was reported in [8,9] to increase with the increase of laser energy density. This had followed directly from the fact that in those experiments the increase of the energy density resulted from the increase of the laser pulse energy, as mentioned above. Therefore, the increased thickness was directly related to the mass of the ablated material from the target ("volume effect"). Our experimental conditions are close to those of Ref. [7]. The highest energy density was achieved when the lens focus was on the target surface in both experiments. When moving closer to the target (defocusing), the laser spot area

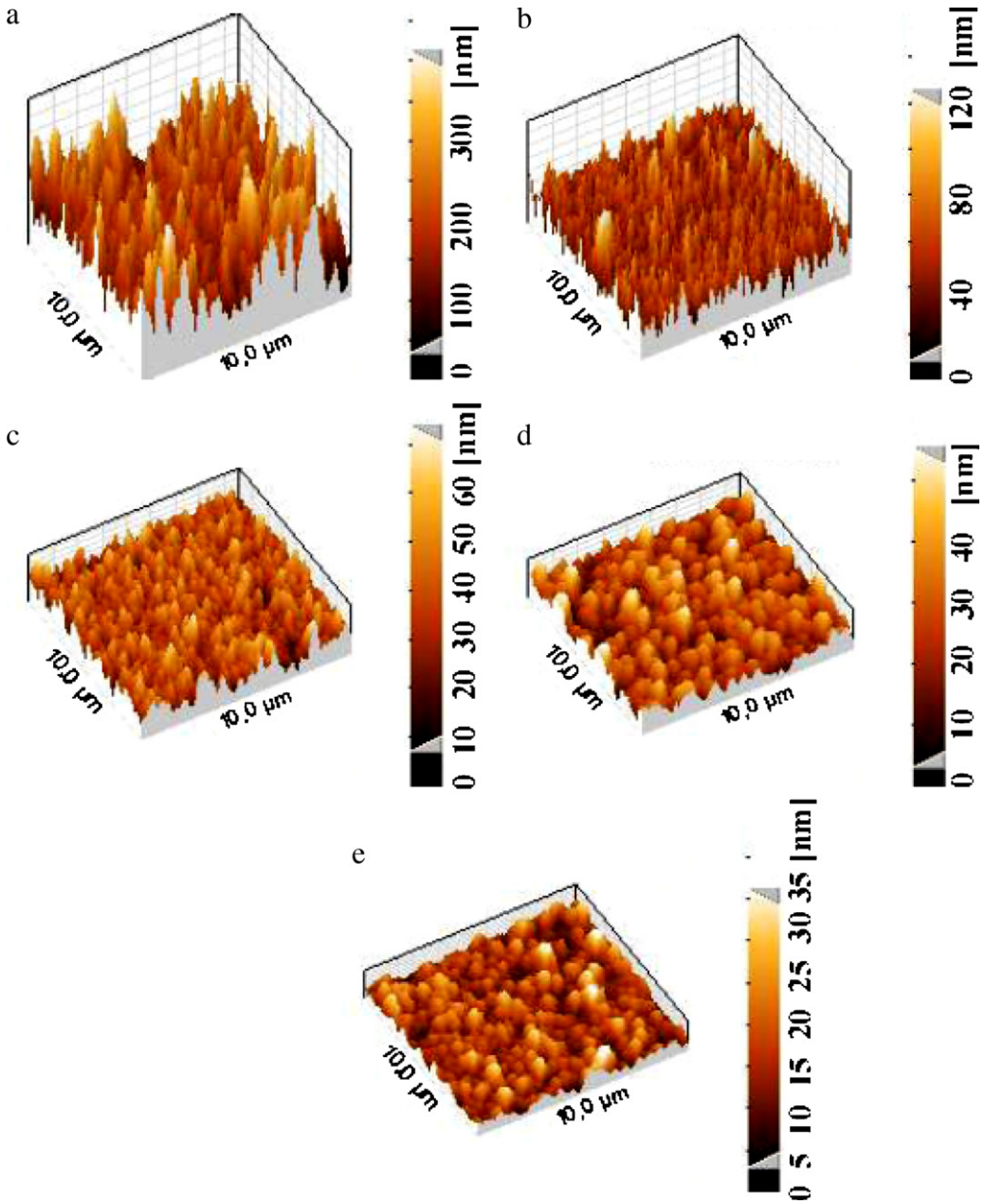

Fig. 5. AFM images of the ZnO films deposited at different laser energy densities: (a) 1.2 J/cm^2, (b) 1.8 J/cm^2, (c) 2.1 J/cm^2, (d) 2.4 J/cm^2, (e) 2.8 J/cm^2.

on the target increased and we observed an increase in the film thickness (see Fig. 7b), as in Ref. [7]. For all films we deposited, the energy density lies therefore well above the ablation threshold in the 1.2–2.8 J/cm^2 range. The thickness therefore scales with the increased spot area and consequently increases because the total number of atoms that arrives at the substrate increase. Due to geometrical constrains in our experiment, we were not able to further defocus the laser beam in order to observe a possible decrease in film thickness as in Ref. [7]. However, it has been also reported by other investigators that there is a critical laser energy density (determined by the spot area) below which the thickness of the film starts to decrease [17]. This means that many atoms have no longer the required kinetic energy to arrive at the substrate.

ZnO is a direct band gap semiconductor; assuming a direct transition between the valence and the conduction bands, the optical band gap (E_g) was estimated from the following equation:

$$(\alpha h\nu)^2 = A(h\nu - E_g) \quad (4)$$

where α is the optical absorption coefficient, h is the Planck's constant, A is a constant and E_g is the band gap.

The transmission data were used to evaluate the absorption coefficient of the ZnO films, according to the following equation:

$$\alpha = \frac{1}{d} \ln\left(\frac{1}{T}\right) \quad (5)$$

where d is the thickness and T is the transmittance of the film. In order to calculate the optical band gap energies of the films, the expression $(ahv)^2$ was plotted as function of the photon energy (hv). By extrapolating the linear portion near the onset of the absorption edge towards the energy axis (at $\alpha = 0$), the optical band gap energy E_g has been estimated as shown in Fig. 8a.

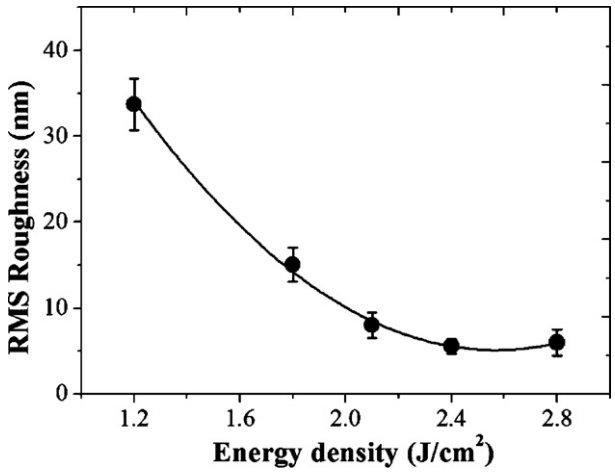

Fig. 6. The root-mean-square (RMS) surface roughness of the deposited ZnO films as a function of the laser energy density.

The optical band gap energies for the deposited ZnO films, were found to be 3.255, 3.263, 3.269, 3.272 and 3.288 eV for energy density values 1.2, 1.8, 2.1, 2.4 and 2.8 J/cm^2, respectively. The corresponding plot is shown in Fig. 8b. The estimated E_g values are close to 3.3 eV which is the value of pure ZnO reported in the literature [18]. The increase (blue shift) of E_g with increasing laser energy density (Fig. 8b) is opposite to the observations of Refs.

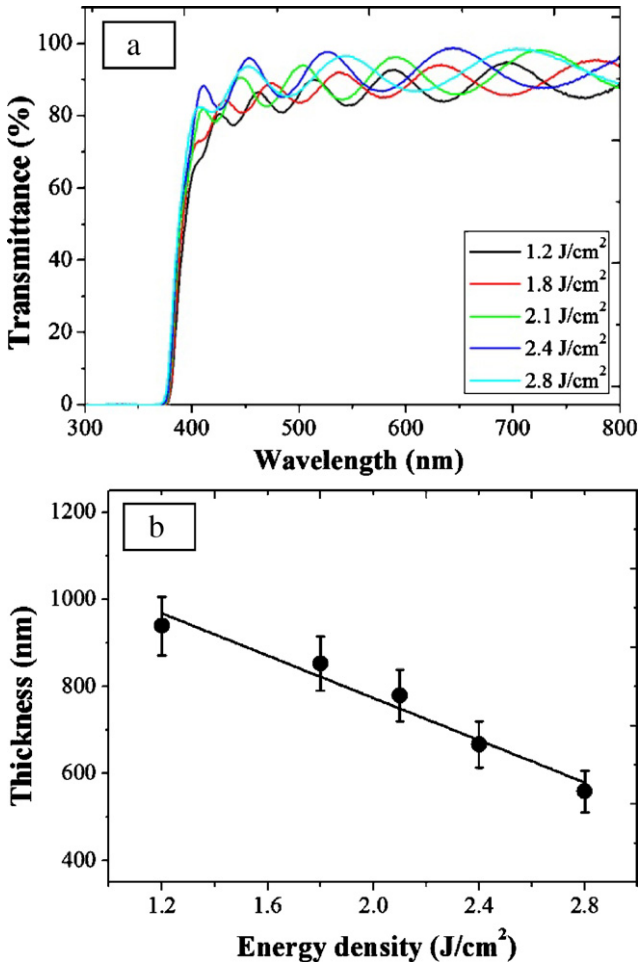

Fig. 7. (a) Transmittance spectra and (b) thickness of the deposited ZnO films as a function of the laser energy density.

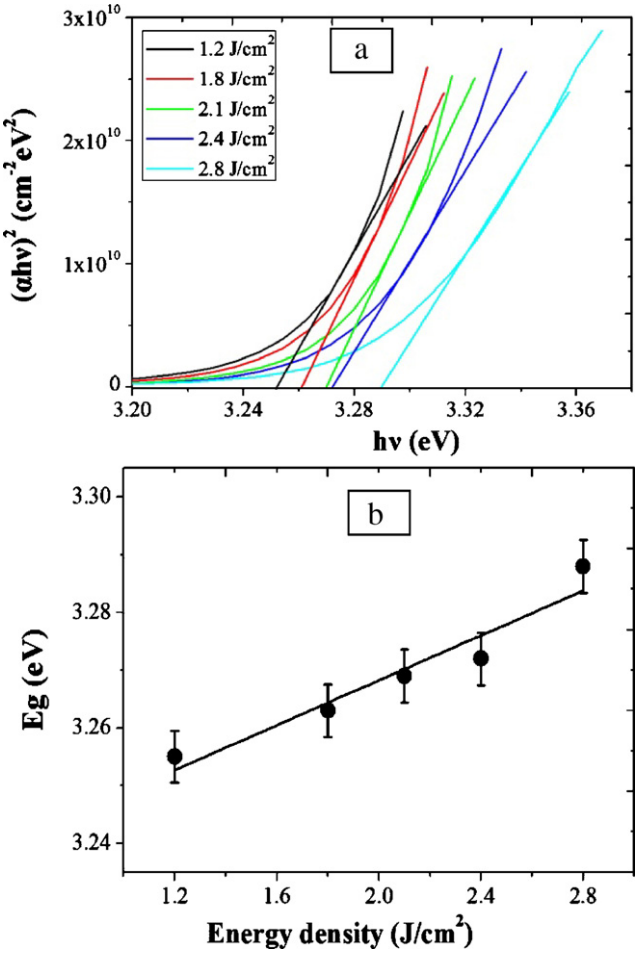

Fig. 8. (a) Plot of $(ahv)^2$ as a function of (hv) for ZnO films deposited with different laser energy density, and (b) laser energy density dependence of the band gap energy for ZnO films.

[8–10] where the energy gap was shown to decrease (red shifted) with increasing energy density. Energy band gap shifts may be due to a number of effects. One such effect is the quantum size effect, which relates the size of the grains with their electrical and optical properties. Indeed, such a blue shift of the band gap with decreasing grain size has been observed by other authors [14,19,20], irrespectively of the composition of their samples. In the present work, the mean diameter of the grain size slightly increases with energy density, see Fig. 4. However, Figs. 5 and 6 show a dramatic decrease of the surface grain size (film roughness), which may account for the E_g blue shift in Fig. 8b. By the same argument, the red shift of the energy band gap, observed in Refs. [8–10], is explained by the increase of the film roughness in those experiments.

A further contribution to the blue shift of E_g can be due to the Burstein–Moss effect [14–16]. As explained in Section 3.3, for high energy densities, the carrier concentration increases which may shift the Fermi energy into the conductivity band. This results to a widening of the optical band gap.

3.3. Electrical properties

The electrical properties of the ZnO films as a function of laser energy density has not been reported thus far [7–10]. The electrical resistivity of the ZnO films at room temperature was measured by the 4-point van der Pauw method and Fig. 9 presents its dependence on the applied energy density. The resistivity increases with an increase of laser energy density up to 2.1 J/cm^2 and then approx-

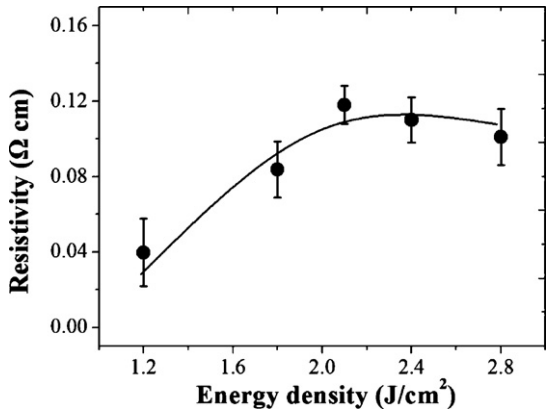

Fig. 9. Resistivity of ZnO films at room temperature as a function of laser energy density.

imately saturates for higher laser energy density. This correlates closely with the thickness dependence on the laser energy density, see Fig. 7b. There is a large number of literature data [21–25], which show that the resistivity decreases with increasing film thickness. Moreover, this is independent of the film composition and growth method. In general, the resistivity ρ is given by $\rho = (N\mu)^{-1}$, where N is the carrier density and μ the carrier mobility. An independent measurement of μ and N (Hall effect) would give more insight into the processes dictated by the variation of the laser energy density, but this possibility was not available.

4. Conclusions

Zinc oxide thin films were deposited on microscope glass substrates by pulsed laser deposition in an oxygen-reactive atmosphere (20 Pa) and a constant value of substrate temperature (300 °C). High quality polycrystalline ZnO films with hexagonal wurtzite structure were grown. The available UV pulsed laser energy was effectively used by changing the focusing lens position and the result was a fine control of the films properties in the applied energy density range. The increase of the laser energy density was found to improve the crystallinity of the ZnO films and slightly increase the average grain size while decreasing the thickness of the film. The surface roughness of the deposited oxide films increased with decreasing laser energy density, probably due to the decreased kinetic energy of the deposited adatoms. The ZnO films exhibited high transmittance of 90% in the visible region at laser energy densities ranging from 1.2 to 2.8 J/cm^2. The energy band gap was slightly increased with the increase of laser energy density. Finally, for the selected experimental conditions, the electrical resistivity of the ZnO films initially increased with increasing laser energy density up to 2.1 J/cm^2 and then remained almost constant.

Acknowledgment

This work has been partially supported from the "Nanostructured organic-inorganic hybrid materials–synthesis, diagnostics and properties" program No. 2005ΣE01330081 of TPCI/NHRF as a "Centre of Excellence", 2005.

References

[1] S. Roy, S. Basu, Bull. Mater. Sci. 25 (2002) 513–515.
[2] Y.I. Alivov, E.V. Kalinina, A.E. Cherenkov, D.C. Look, B.M. Ataev, A.K. Omaev, M.V. Chukichev, D.M. Bagnall, Appl. Phys. Lett. 83 (2003) 4719–4721.
[3] J.C. Lee, K.H. Kang, S.K. Kim, K.H. Yoon, I.J. Park, J. Song, Sol. Energy Mater. Sol. C 64 (2000) 185–195.
[4] D.B. Chrisey, G.K. Hubler, Pulsed Laser Deposition of Thin Films, Wiley, New York, 1994.
[5] M. Girtan, M. Kompitsas, R. Mallet, I. Fasaki, Eur. Phys. J. Appl. Phys. 51 (2010) 33212.
[6] M.G. Tsoutsouva, C.N. Panagopoulos, D. Papadimitriou, I. Fasaki, M. Kompitsas, Mater. Sci. Eng. B (2010), in press. doi:10.1016/j.mseb.2010.03.059.
[7] M. Liu, G. Sun, Z.G. Zhang, X.Q. Wei, C.S. Chen, C.S. Xue, B.Y. Man, Eur. Phys. J. Appl. Phys. 34/2 (2006) 73–76.
[8] B.L. Zhu, X.Z. Zhao, F.H. Su, G.H. Li, X.G. Wu, J. Wu, R. Wu, J. Liu, Physica B 396 (2007) 95–101.
[9] B.D. Ngom, T. Mpahane, N. Manyala, O. Nemraoui, U. Buttner, J.B. Kana, A.Y. Fasasi, M. Maaza, A.C. Beye, Appl. Surf. Sci. 255 (2009) 4153–4158.
[10] S. Venkatachalam, Y. Kanno, Curr. Appl. Phys. 9 (2009) 1232–1236.
[11] J.C. Manifacier, J. Gasiot, J.P. Fillard, J. Phys. E: Sci. Instrum. 9 (1976) 1002–1004.
[12] E. Dumont, B. Dugnoille, S. Bienfait, Thin Solid Films 353 (1999) 93–99.
[13] X.L. Tong, D.S. Jiang, L. Liu, M.Z. Luo, Opt. Commun. 270 (2007) 356–360.
[14] A.Y. Fasasi, M. Maaza, E.G. Rohwer, D. Knoessen, Ch. Theron, A. Leitch, U. Buttner, Thin Solid Films 516 (8) (2007) 6226–6232.
[15] H. Kim, J.S. Horwitz, G. Kushto, A. Pique, Z.H. Kafafi, C.M. Gilmore, D.B. Chrisey, J. Appl. Phys. 88 (2000) 6021–6025.
[16] H. Kim, J.S. Horwitz, A. Pique, C.M. Gilmore, D.B. Chrisey, Appl. Phys. A 69 (Suppl.) (1999) S447–S450.
[17] T. Ohnishi, H. Koinuma, M. Lippmaa, Appl. Surf. Sci. 252 (2006) 2466–2471.
[18] Y.I. Özgür, C. Alivov, A. Liu, M.A. Teke, S. Reshchikov, V. Dogan, S.-J. Avrutin, H. Cho, Morkoc, J. Appl. Phys. 98 (2005) 041301–42103.
[19] J. Lee, T. Tsakalakos, Nanostruct. Mater. 8 (1997) 381–398.
[20] L. Escobar-Alarcoón, A. Arrieta, E. Camps, S. Muhl, S. Rodil, E. Vigueras-Santiago, Appl. Surf. Sci. 254 (2007) 412–441.
[21] M.Y. Lim, W.M.M. Yunus, Z.A. Talib, A. Kassim, C.F. Dee, A. Ismail, Am. J. Eng. Appl. Sci. 3 (2010) 64–67.
[22] M. Mosleh, N. Pryds, P.V. Hendriksen, Mater. Sci. Eng. B 144 (2007) 38–42.
[23] K. Ulutaş, D. 1, Y. Değer, Skarlatos, Phys. Stat. Sol. (a) 203 (2006) 2432–2437.
[24] G. Wakefield, P.J. Dobson, Y.Y. Foo, A. Loni, A. Simons, J.L. Hutchison, Semicond. Sci. Technol. 12 (1997) 1304–1309.
[25] A.I. Ivashchenko, I.I. Kerner, G.A. Kiosse, I.Yu. Maronchuk, Thin Solid Films 303 (1997) 292–294.